

ESI for

Local hydrophobic environment in metal–organic framework for boosting photocatalytic CO₂ reduction in the presence of water

Ning-Yu Huang, Xue-Wen Zhang, Yu-Zhi Xu, Pei-Qin Liao* and Xiao-Ming Chen

MOE Key Laboratory of Bioinorganic and Synthetic Chemistry, School of Chemistry, Sun Yat-Sen University, Guangzhou 510275, China

*E-mail: liaopq3@mail.sysu.edu.cn

Supplementary Index

Experimental details.

Figure S1. PXRD patterns of MOF-525, MCF-55 and VPI-100(Ni).

Figure S2. The optimized structures of *cis*-H₄tactmb, *trans*-H₄tactmb and H₄TCPP-H₂.

Figure S3. PXRD patterns of MCF-55-Co and MCF-55-Ni after immersed in different solutions.

Figure S4. XPS spectra of MCF-55-Co and MCF-55-Ni.

Figure S5. H₂ production rates of photocatalytic CO₂ reduction by using catalysts MCF-55-Ni and MCF-55-Co as catalysts.

Figure S6. The GC profiles for the gaseous products from the photocatalytic CO₂ reduction by using MCF-55-Ni as catalysts.

Figure S7. SEM images of the MCF-55-Co and MCF-55-Ni.

Figure S8. TG curves of MCF-55-Co and MCF-55-Ni.

Figure S9. CO₂ adsorption isotherms of MCF-55-Ni at 195 K.

Figure S10. Mass spectra of reaction products of a photocatalytic reaction using MCF-55-Ni as the catalyst.

Figure S11. PXRD patterns of MCF-55-Ni before and after photocatalytic reaction.

Figure S12. CO production TOFs of repeated photocatalytic CO₂ reduction reactions by using [(H₄tactmb-Ni)(Cl)₂] as catalyst.

Table S1. ICP-AES results of MCF-55-M (M = Ni, Co).

Table S2. Comparison of the photocatalytic CO₂ reduction performances of MCF-55-Ni and other MOF catalysts.

Table S3. Summary of photocatalytic CO₂ reduction experiments.

Experimental section

Materials and Methods. All reagents were commercially available and used without further purification. 1,4,7,10-tetraazacyclododecane-*N,N',N'',N'''*-tetra-*p*-methylbenzoic acid (H₄tactmb) was synthesized according to literature method.^[*CrystEngComm*, 2012, 14, 6115.] X-ray photoelectron spectroscopy (XPS) measurements were performed with a VG Scientific ESCALAB 250 instrument. Powder X-ray diffraction (PXRD) patterns were collected on a Bruker D8-Advance diffractometer with Cu K α radiation and a LynxEye detector. Thermogravimetry (TG) analyses were performed on a TA Q50 thermogravimetric analyzer under nitrogen gas at a heating rate of 10 °C/min. Scanning electron microscope (SEM) images were obtained from an Ultra-high Resolution electron microscope (FE-SEM, SU8010). Inductively coupled plasma-atomic emission spectrometry (ICPAES) was performed on an IRIS(HR) spectrometer (TJA, USA). Gas sorption isotherms were measured on a Micromeritics ASAP 2020M instrument. Before the sorption experiments, the as-synthesized samples were first solvent exchanged by MeOH, and then activated for 12 h under vacuum. CO₂ (99.999%) was used for all measurements. The temperature was controlled by an acetone-dry ice bath (195 K).

Synthesis of [Zr₆(OH)₄O₄(tactmb)₃] (denoted as MCF-55). A mixture of ZrCl₄ (23.3 mg, 0.1 mmol), H₄tactmb (35.4 mg, 0.05 mmol), benzoic acid (BA, 1.2 g) and *N,N*-Dimethylformamide (DMF, 4.0 mL) were ultrasonically dissolved in a Pyrex vial, heated in an oven at 100 °C for 72 h, and then cooled to room temperature at a rate of 10 °C h⁻¹, giving small colorless block-shape crystals. The resultant product were washed with MeOH for three times and collected by filtration (yield 70%).

Synthesis of [Zr₆(OH)₄O₄(tactmb-Co)₃(Cl)₆] (denoted as MCF-55-Co). CoCl₂·6H₂O (60 mg) and MCF-55 (50 mg) was added to a 10 mL DMF solution, the solution was heated at 100 °C for 48 hours. The microcrystalline powder was collected by filtration and washed with DMF for three times. The DMF within the pores of the samples was then exchanged with methanol (5 × 30 mL) over a five-day period. Finally, the methanol was removed by evacuation for 24 hours.

Synthesis of [Zr₆(OH)₄O₄(tactmb-Ni)₃(Cl)₆] (denoted as MCF-55-Ni). The synthesis process of MCF-55-Ni is much similar to that of MCF-55-Co, except that NiCl₂·6H₂O (60 mg) was used to replace the CoCl₂·6H₂O (60 mg).

Photocatalytic Measurements. Microcrystals of the MOF catalysts (5 mg) were dispersed in water (5 mL) with ultrasonication for 30 min, and the amount of catalyst was determined by the volume of the suspension. The photocatalytic CO₂ reduction was conducted under 1 atm of a certain atmosphere (pure CO₂ or CO₂/Ar mixed gas, v/v = 10:90) at 25 °C in a 16-mL reactor containing catalyst (n(Co²⁺) = 30 nmol), [Ru(phen)₃]Cl₂·6H₂O (2 μmol), TEOA (0.3 M), and CH₃CN/H₂O (v/v = 4:1, 5 mL). The reaction mixture was continuously stirred with a magnetic bar and irradiated under a LED light (λ = 450 nm). The generated gas samples were analyzed by an Agilent 7820A gas chromatography equipped with a thermal conductivity detector (TCD) and a TDX-01 packed column. The oven temperature was held constant at 60 °C, and the inlet and detector temperature were set at 80 °C and 200 °C, respectively. The products in the liquid phase of the photocatalytic CO₂ reaction were analyzed by a Thermo Scientific Dionex ion chromatography (IC) system 5000 with an AS11HC column. Each photocatalytic reaction was repeated at least three times to confirm the reliability of the data.

The concentration of Ni in the filtrate was detected by the inductively coupled plasma–mass spectrometry. After photocatalytic CO₂ reduction (10 nmol catalysts in 5 mL solution), 3 mL of the filtrate was digested and diluted to 10 mL for tests. The concentration of Ni in the concentrated filtrate was detected as 1.07 ng/mL. Therefore, the dissolved Ni ions of the MOF was $(1.07 \text{ ng mL}^{-1} \times 10 \text{ mL}) / (6 \text{ nmol} \times 3 \times 59 \text{ g mol}^{-1}) = 1.01\%$.

Computational Methods. All simulations/calculations were performed by the Materials Studio 5.0 package. All energies were calculated by the periodic density functional theory (PDFT) method by the Dmol3 module. Full geometry optimizations with fixed cell parameters were performed to the systems. The widely used generalized gradient approximation (GGA) with the Perdew-Burke-Ernzerhof (PBE) functional and the double numerical plus d-functions (DNP) basis set, TS for DFT-D correction as well as the Effective Core Potentials (ECP) were used. The energy, force and displacement convergence criteria were set as 1×10^{-5} Ha, 2×10^{-3} Ha and 5×10^{-3} Å, respectively.

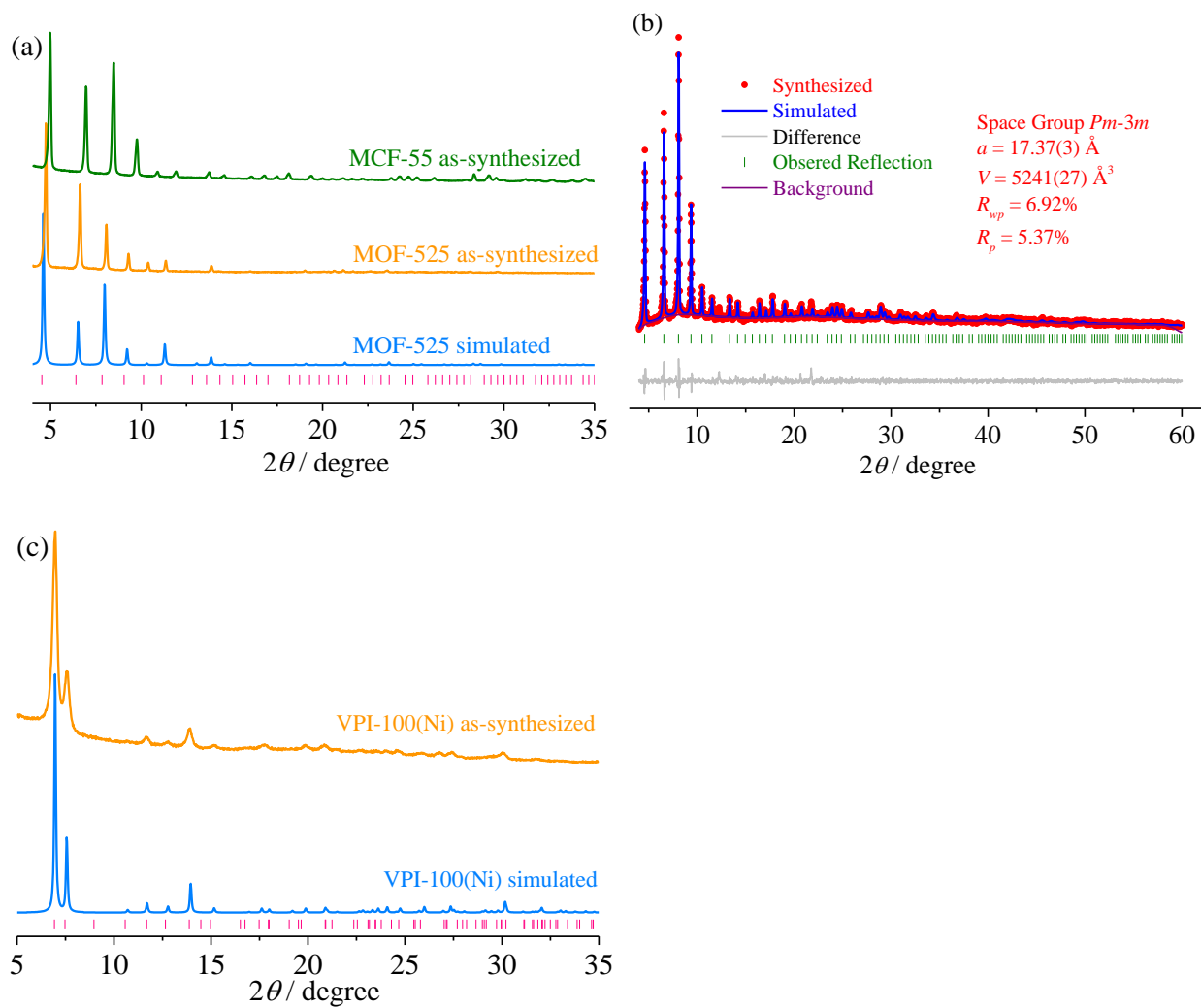


Figure S1. (a) PXRD patterns of MOF-525 and MCF-55. (b) Rietveld refinement results of MCF-55. (c) PXRD patterns of VPI-100(Ni).

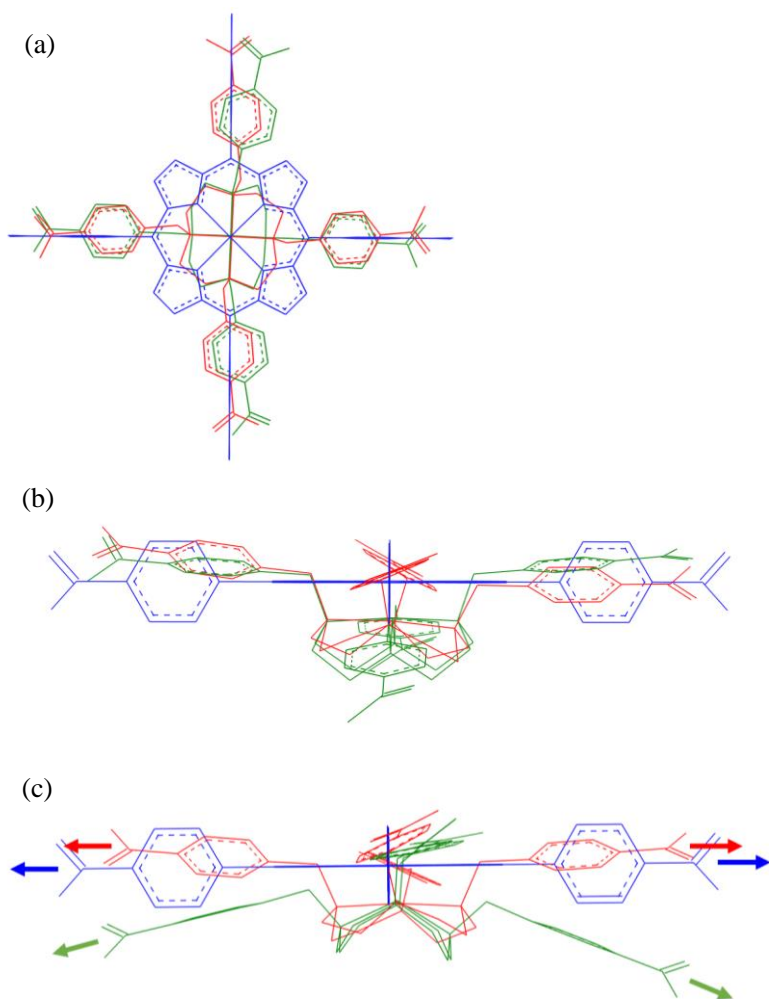


Figure S2. (a) Top and (b-c) side views of the optimized structures of *cis*-H₄tactmb (green), *trans*-H₄tactmb (red) and H₄TCPP-H₂ (blue). H atoms are omitted for clarity.

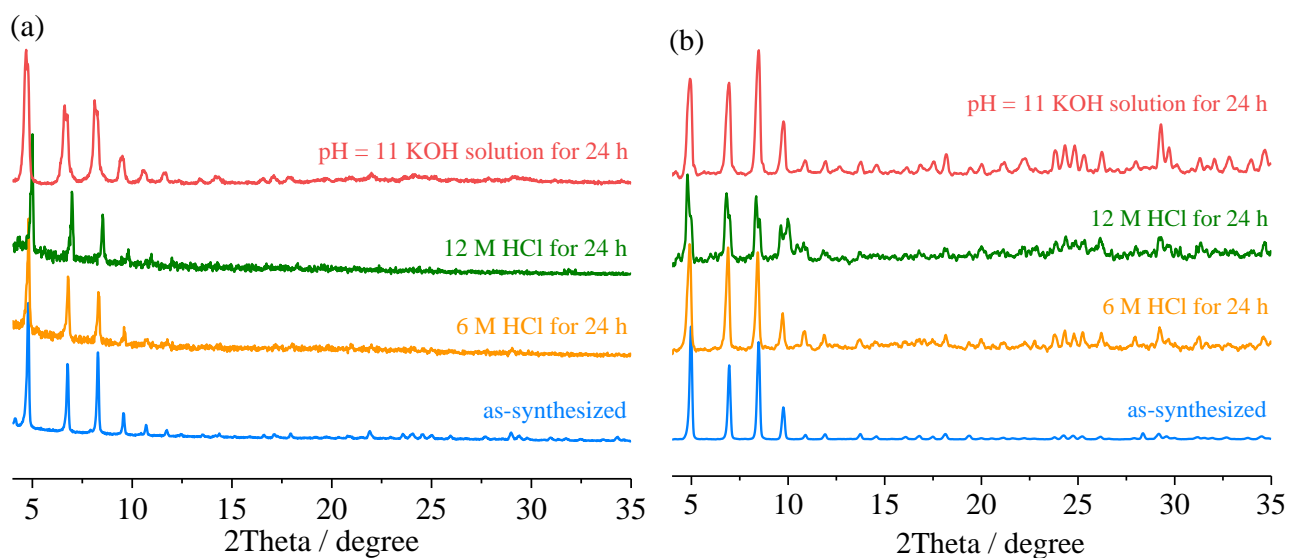


Figure S3. PXRD patterns of (a) MCF-55-Ni and (b) MCF-55-Co after immersed in different solutions.

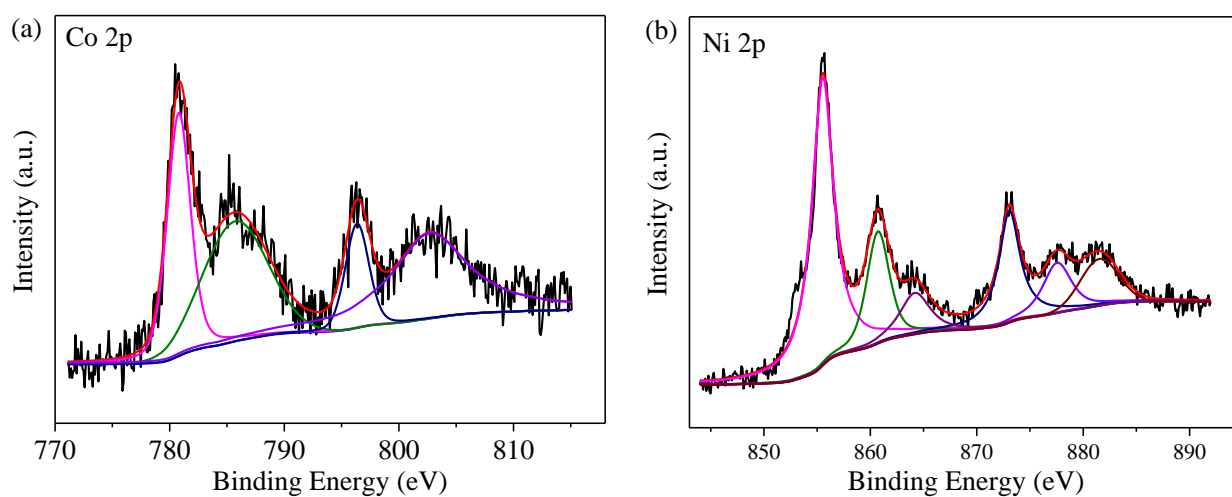


Figure S4. XPS Co2p spectrum of MCF-55-Co and Ni2p spectrum of MCF-55-Ni.

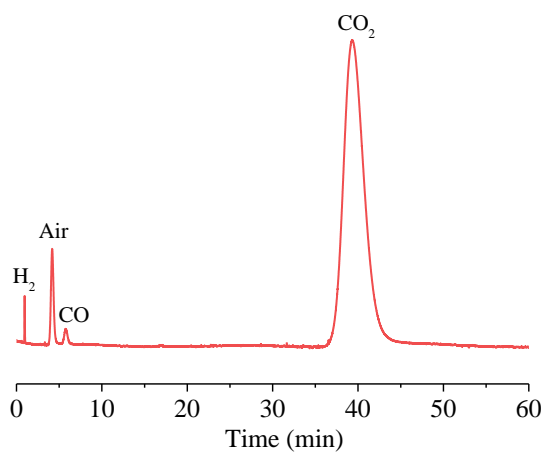


Figure S5. The GC profiles for the gaseous products from the photocatalytic CO₂ reduction by using MCF-55-Ni as catalysts.

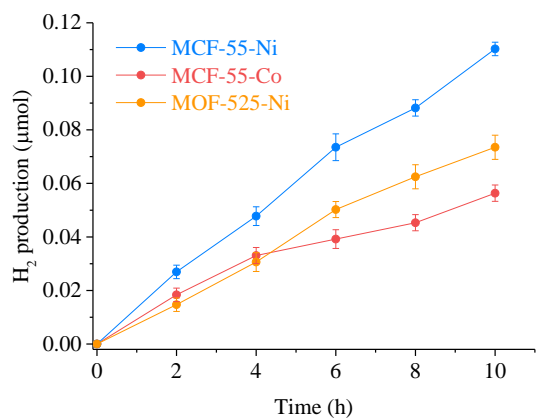


Figure S6. H₂ production rates of photocatalytic CO₂ reduction by using catalysts MCF-55-Ni, MCF-55-Co and MOF-525-Ni.

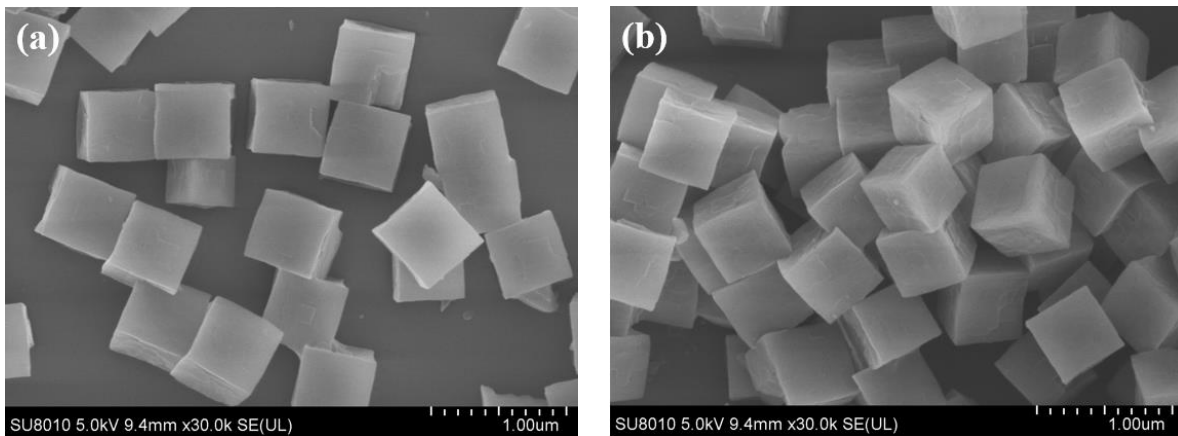


Figure S7. SEM images of the (a) MCF-55-Co and (b) MCF-55-Ni. According to the SEM images, the particle sizes of MCF-55-Co and MCF-55-Ni are similar, meaning that the different photocatalytic activities are not because of the particle sizes.

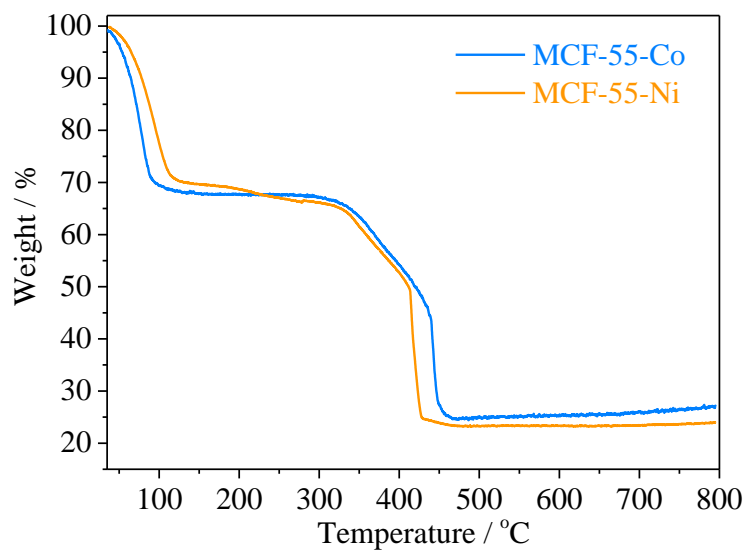


Figure S8. TG curves of MCF-55-Co and MCF-55-Ni.

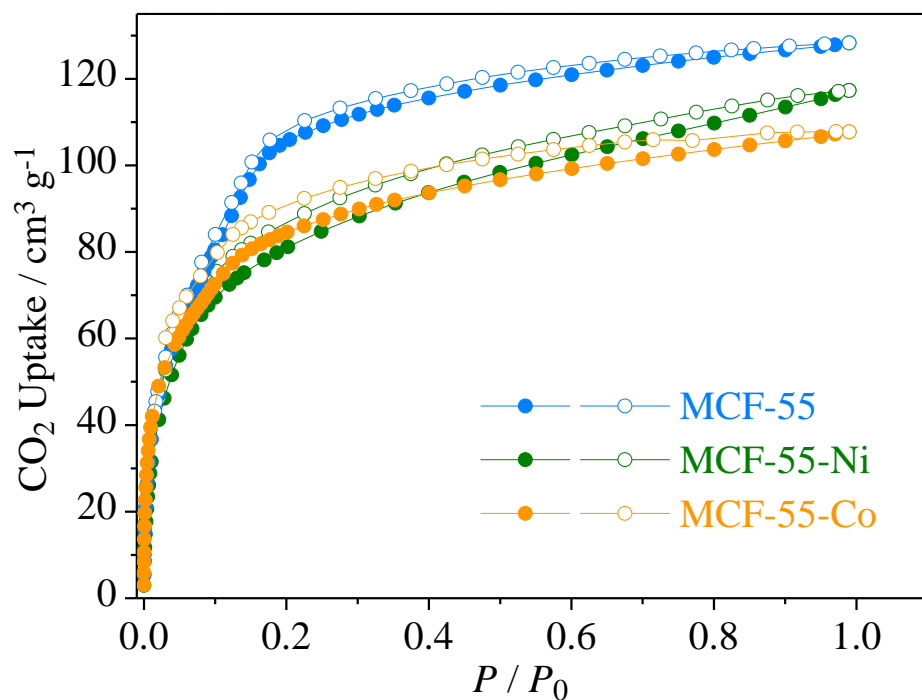


Figure S9. CO₂ adsorption (solid symbols) and desorption (open symbols) isotherms of MCF-55, MCF-55-Ni and MCF-55-Co at 195 K.

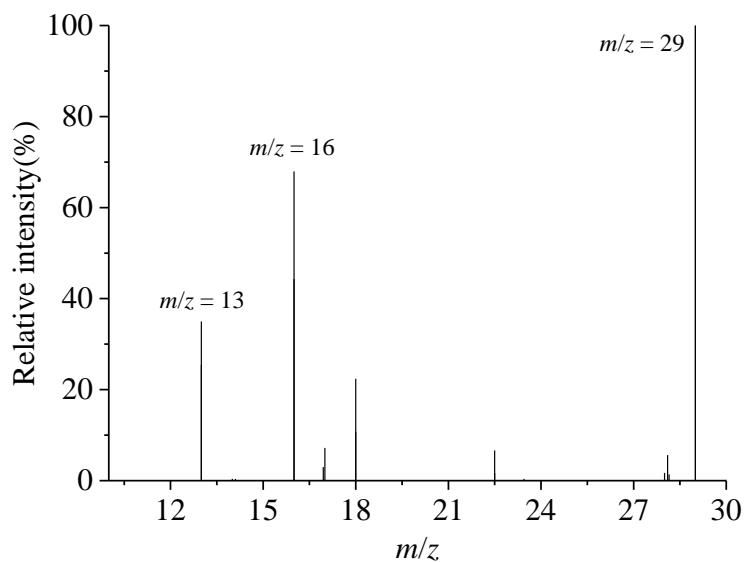


Figure S10. Mass spectra of reaction products of photocatalytic CO₂ reduction using MCF-55-Ni as the catalyst by using ¹³CO₂ as the gas environment. The peak at $m/z = 29.1$ can be assigned to and ¹³CO.

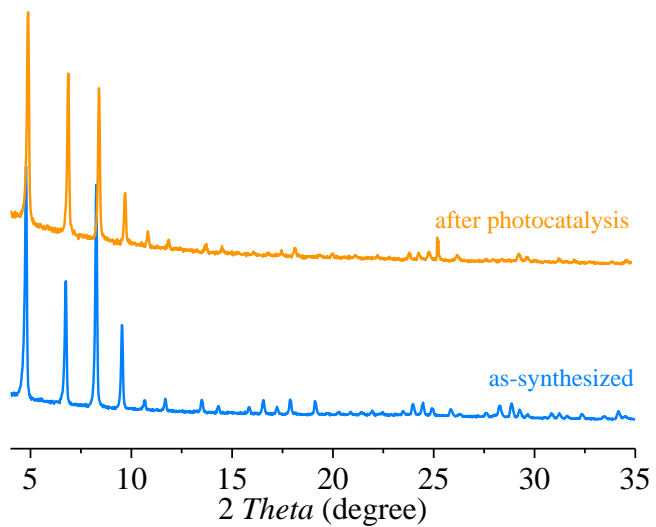


Figure S11. PXRD patterns of MCF-55-Ni before and after photocatalytic reaction.

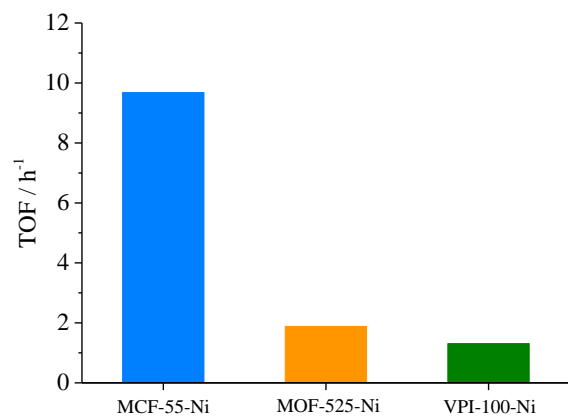


Figure S12. CO production TOFs of MCF-55-Ni, MOF-525-Ni and VPI-100-Ni.

Table S1. ICP-AES results of MCF-55-M (M = Ni, Co).

Materials	n/mmol·L⁻¹		Zr:M		Ratio
	Zr	M	Theoretical	Experimental	
MCF-55-Ni	0.0438	0.0215	2:1	2.04:1	98.7%
MCF-55-Ni21%	0.0603	0.0064	2:1	9.42:1	21.2%
MCF-55-Ni1.7%	0.0690	0.00059	2:1	116.9:1	1.7%
MCF-55-Co	0.0709	0.0320	2:1	2.22:1	90.1%

Table S2. Comparison of the photocatalytic activities of **MCF-55-M** and MOF catalysts.

Material	Solvent	λ	Major Products	Generation Rate / $\mu\text{mol g}^{-1} \text{h}^{-1}$	TOF/ h^{-1}	TON	CO Selectivity	Ref.
MCF-55-Ni	MeCN-H ₂ O (4:1 v/v)	> 450 nm	CO, H ₂	CO 9377	CO 9.69	CO >448	96.1%	This work
MCF-55-21%Ni	MeCN-H ₂ O (4:1 v/v)	> 450 nm	CO, H ₂	CO 4551	CO 22.2	CO >88.8	97.1%	
MCF-55-1.7%Ni	MeCN-H ₂ O (4:1 v/v)	> 450 nm	CO, H ₂	CO 1214	CO 73.8	CO >295	95.9%	
MCF-55-Co	MeCN-H ₂ O (4:1 v/v)	> 450 nm	CO, H ₂	CO 7097	CO 7.41	CO >37.1	96.5%	
MOF-525-Ni	MeCN-H ₂ O (4:1 v/v)	> 450 nm	CO, H ₂	CO 1674	CO 1.76	CO >17.3	86.9%	
MOF-525-Co	MeCN	> 400 nm	CO, CH ₄	CO 200.6	CO 0.216	/	84.6%	<i>Angew. Chem. Int. Ed.</i> 2016 , <i>55</i> , 14310
ZrPP-1-Co	MeCN	> 420 nm	CO, CH ₄	CO 14	/	/	96.4%	<i>Adv. Mater.</i> 2018 , <i>30</i> , 1704388.
PCN-222	MeCN	> 420 nm	HCOO ⁻	/	0.0717	/	/	<i>J. Am. Chem. Soc.</i> , 2015 , <i>137</i> , 13440
Co-ZIF-9	MeCN-H ₂ O (4:1 v/v)	> 420 nm	CO, H ₂	/	CO 104.5	CO 89.6	58.3%	<i>Angew. Chem. Int. Ed.</i> 2014 , <i>53</i> , 1034
Co-MOF-74	MeCN-H ₂ O (4:1 v/v)	> 420 nm	CO, H ₂	/	/	CO 23.8	61.6%	
MAF-X27l-OH	MeCN-H ₂ O (4:1 v/v)	> 420 nm	CO, H ₂	/	CO 212.4	/	98.2%	<i>J. Am. Chem. Soc.</i> , 2018 , <i>140</i> , 38
Hf ₁₂ -Ru-Re	MeCN	> 400 nm	CO, HCOOH	/	/	CO 8613	98%	<i>J. Am. Chem. Soc.</i> , 2018 , <i>140</i> , 12369
Ni MOLs	MeCN-H ₂ O (3:2 v/v)	> 400 nm	CO, H ₂	CO 12500	/	/	97.8%	<i>Angew. Chem. Int. Ed.</i> 2018 , <i>57</i> , 1

Table S3. Summary of photocatalytic CO₂ reduction experiments.

	H ₂ / μmol	TOF / h ⁻¹	CO / μmol	TOF / h ⁻¹	CO selectivity
MCF-55-Ni	0.15	0.63	2.71	12.96	95.41%
Without catalyst	0.01	0.04	0.33	1.10	96.39%
Without photosensitizer	0.01	0.02	0	0	0
Without sacrificial agent	0.04	0.12	0	0	0
Without light	0.01	0.02	0	0	0
Using dry CH ₃ CN to replace CH ₃ CN/H ₂ O mixture	0.02	0.07	0	0	0
Using H ₂ O to replace CH ₃ CN/H ₂ O mixture	0.01	0	0	0	0
Using filtrate to replace catalyst	0.01	0	0	0	0

*Basic reaction condition: [Ru(phen)₃]Cl₂·6H₂O (2 μmol), catalysts (30 nmol on the basis of Ni), solvent (5 mL, CH₃CN/H₂O = 4:1), triethanolamine (TEOA, 1.5 mmol), LED light (λ = 450 nm), 25 °C, 1.0 atm.